Free Energy Perturbation Study of Octanol/Water Partition Coefficients: Comparison with Continuum GB/SA Calculations

Scott A. Best,[†,‡] Kenneth M. Merz, Jr.,*[,†] and Charles H. Reynolds[‡]

Department of Chemistry, The Pennsylvania State University, University Park, Pennsylvania 16802, and Rohm and Haas Company, 727 Norristown Road, Spring House, Pennsylvania 19477

Received: October 27, 1998

Molecular dynamics (MD) free energy perturbation (FEP) simulations were carried out in order to obtain insights into the structures and dynamics of a series of small organic solutes in water and water-saturated 1-octanol. Relative free energies of solvation were computed for each solute in both solvents, and these results were used to estimate the relative octanol/water partition coefficients (log P_{ow}). The relative octanol/water partition coefficients were in good agreement with experimental log P_{ow} values (average unsigned error = 0.74 log units), if one omits the acetamide−acetone simulation which proved problematic. Partition coefficients were also calculated using the newly developed GB/SA octanol continuum solvation model in order to compare the MD-FEP and continuum model results. Interestingly, the computationally much more efficient GB/SA calculations proved to be more accurate (average unsigned error in log P_{ow} = 0.50 log units) than FEP for this set of 12 solutes.

Introduction

Many important biochemical interactions occur in both aqueous and lipophilic environments, for example, the interior of a biological membrane or the active site of an enzyme. The nature of the surrounding medium can have a profound effect on biological processes such as receptor−ligand binding, reactivity, or transport of molecules across a biomembrane.[1−5] In addition, numerous other properties, including bioavailability, skin permeability, toxicity, and environmental fate, have all been successfully related to the differential solubility of solutes in aqueous and organic solvents.[1−6] It is, therefore, very important to understand solute−solvent interactions in both aqueous (hydrophilic) and organic (lipophilic) solvents. Most theoretical studies of solvent effects have concentrated on water[7−14] because water is the most important solvent in biological systems.

Arguably, the most significant organic solvent for the study of biological systems is 1-octanol (henceforth referred to as octanol). Octanol has been widely used as a surrogate for much more complicated systems such as lipid molecules that comprise biological membranes. In particular, the partition coefficient[15] for distribution of a solute between octanol and water, log P_{ow}, is widely used to predict pharmacokinetic properties such as bioavailability, transport, and elimination.[1−6] While octanol is primarily lipophilic (oily) in nature by virtue of its lengthy alkyl tail, it also possesses a polar head group that provides for local regions in the solvent that are capable of hydrogen bonding, and might be characterized as being relatively hydrophilic. This amphipathic character gives octanol characteristics that are similar to those of lipids in biological membranes, or at least that has been the traditional argument for using log P_{ow} as an indicator for membrane transport. Recent octanol simulations of Debolt and Kollman support this view by showing that water-saturated octanol contains micellar-like regions.[16] The propensity of octanol to form solvent structures with both locally polar (hydrophilic) and nonpolar (lipophilic) regions is lacking in simpler organic solvents, such as $CHCl_3$ or long-chain hydrocarbons,[17−22] and is most likely the reason these solvents have been less useful for predicting pharmacokinetic properties.

Numerous attempts have been made to simulate the interaction of small solutes with biological membranes using a variety of model systems ranging from lipid bilayers[23−29] to the use of long-chain hydrocarbons.[17−22] Unfortunately, simulations for explicit lipid bilayer models are computationally very expensive and simple hydrocarbon models consistently break down when compared to experiment.[30−32] The ability to directly model solute−solvent interactions in octanol, beyond being theoretically interesting in light of the discussion above, would have great practical value given the important role lipophilicity often plays in rational drug design.

A number of computational methods[1,2,33] have been developed to predict partition coefficients. Most of these models are based on group additivity using either fragment or atom-derived group equivalents.[34−39] Other methods employ an empirically derived quantitative structure−property (QSPR) model that relates log P_{ow} to some set of calculated molecular properties.[40−48] The advantages of these methods are that they are very fast, allowing them to be applied to large databases of structures, in many cases they require only 2-D molecular connectivities, and can be very accurate for molecules with well-defined group equivalents. The disadvantages of group equivalent, or QSPR methods are that they require large numbers of empirically derived parameters, they cannot be used to examine conformational effects in the solute, and many times no parameters exist for calculating the log P_{ow}, of new chemical classes.

Molecular dynamics (MD) and Monte Carlo (MC) simulations as well as continuum solvation models hold promise for calculating partition coefficients directly without resorting to completely empirical schemes. In addition, simulations can provide molecular level insight into the factors driving the partitioning of solutes between two solvents that are otherwise

* Author to whom correspondence should be addressed.
† The Pennsylvania State University.
‡ Rohm and Haas Company.

10.1021/jp984215v CCC: $18.00
Published on Web 01/13/1999

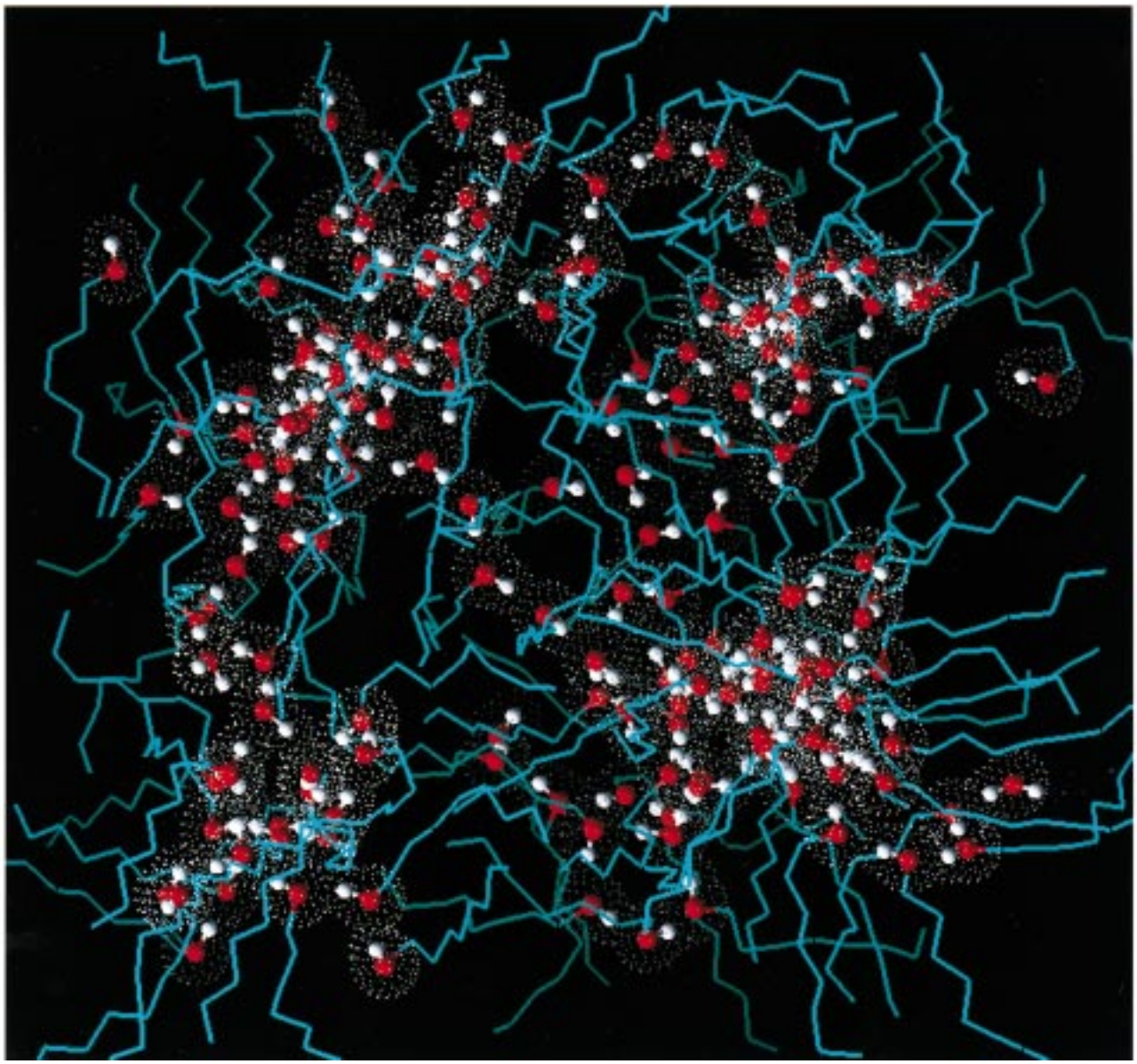

Figure 1. Illustration of the polar and hydrophobic regions in water-saturated octanol. The waters and hydroxyls are colored by atom, and the polar regions are outlined with white van der Waals surfaces. The hydrophobic octanol tails are represented as simple stick figures.

unavailable. Attempts have been made to calculate log P_{ow} values directly using either simulations that include explicit solvent[16,33,49−56] or continuum solvation methods such as COSMO,[45,57] SMX,[58−61] or generalized Born/surface area model (GB/SA).[62,63] For example, the GB/SA method has recently been parameterized for octanol, enabling direct calculation of octanol/water partition coefficients using this method.[62] Direct calculation of octanol/water partition coefficients offers the promise of calculating accurate partition coefficients for a wide variety of molecules with a degree of generality not available from the fragment-based methods.

In this study, MD free energy perturbation (FEP) calculations have been utilized to gain insight into the structure and thermodynamics of a series of small organic molecules in a box of water-saturated octanol. Water-saturated octanol is used rather than neat octanol because octanol readily absorbs a significant amount of water. For this reason, experimental measurements of octanol/water partition coefficients are always conducted using octanol that has first been saturated with water. We have employed a water-saturated octanol model that is based on OPLS and TIP3P water.[64,65] This is a slight departure from the previous study[16] of water-saturated octanol that used OPLS and SPC water.

One of the principal aims of this study was to evaluate the ability of FEP simulations to predict octanol/water partition coefficients. Partition coefficients were estimated from the differences between the aqueous and water-saturated octanol free energies of solvation. These predicted log P_{ow} values were compared to experimentally determined partition coefficients to examine the reliability of the method. The results were also compared to log P_{ow} values that were calculated using our octanol GB/SA model[62] in order to evaluate the advantages and deficiencies associated with each model.

Construction of Models

A box of water-saturated octanol molecules was constructed by randomly placing octanol and TIP3P water molecules in a specified volume space. The molecules were randomly arranged in the box with a 2.2 Å tolerance between adjacent molecules. The model consisted of 125 octanol molecules and 42 water

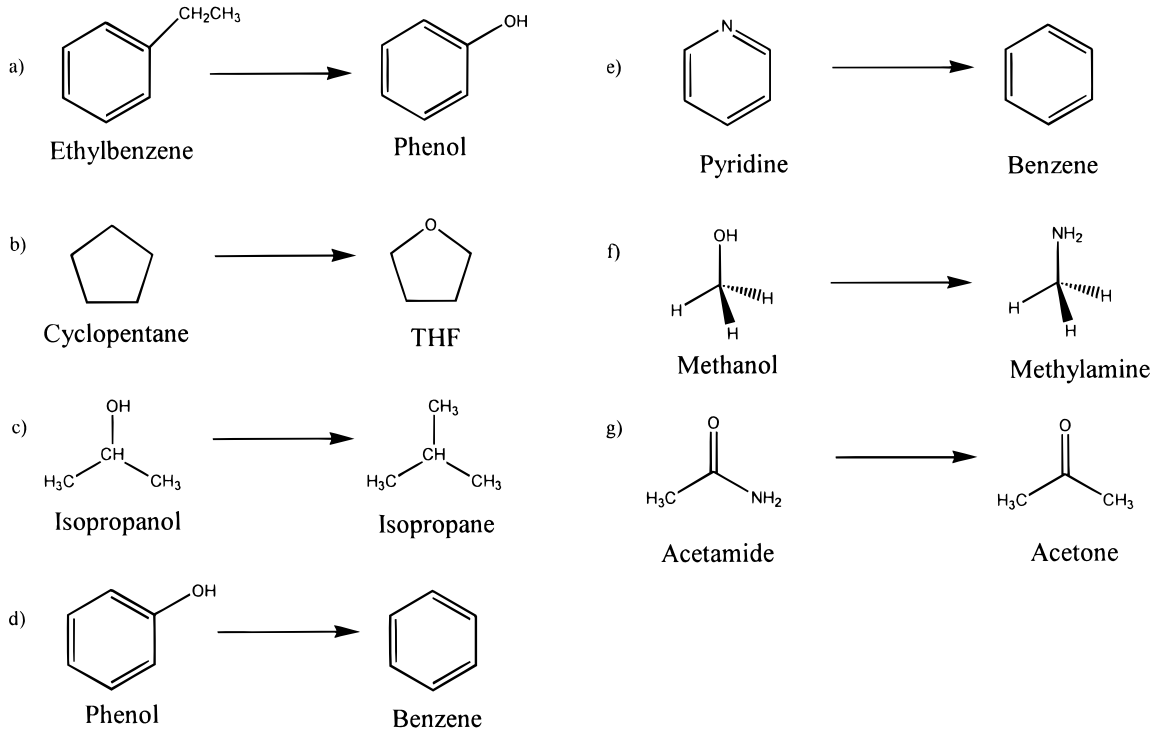

Figure 2. Free energy perturbations involving small molecules that were completed in both water and water-saturated octanol. The solutes were modeled using the united atom OPLS[64] model incorporated in AMBER 4.1.[70,84] Phenol, pyridine, and benzene were modeled on the basis of Jorgensen's all-atom OPLS model.[71−74]

molecules which corresponds to a mole fraction of water, X_{wat}, of 0.252. It has been shown experimentally that the mole fraction of water in a fully saturated octanol solution is temperature dependent and can vary significantly. For example, X_{wat} is 0.245 at 20 °C, 0.255 at 25 °C, and 0.290 at 30 °C.[16] The simulations that were carried out in this study were run at 27 °C so that the model which was constructed is slightly less than a fully saturated solution.

The water-saturated octanol model was initially equilibrated for approximately 900 ps, and coordinates were collected for an additional 450 ps in order to examine the structure and dynamics of the solvent mixture. Visual inspection showed the development of inverted micellar regions within the solvent box as the polar head groups of the octanol solvent molecules interacted with the water molecules (Figure 1). In order to compare with experimental results, as well as with the results of previous simulations, various physical properties associated with the solvent mixture were calculated. The calculated properties included the system volume, self-diffusion coefficients, and radial distribution functions (RDFs) for the solvent mixture.

The free energies of solvation for both the aqueous phase as well as in the water- saturated octanol solvent mixture were computed for a series of small organic molecules utilizing FEP simulations. (A detailed description of the FEP method will not be discussed here; the reader is referred to the numerous reviews pertaining to this subject.[10,53,66−69]). In performing these simulations, each of the solutes was incorporated into the equilibrated octanol/water box. In placing the solutes into the solvent box, a cavity was initially created in the center of the box by removing three octanol molecules and one water molecule. In creating this cavity, X_{wat} essentially remained constant so it was thought that removing these solvent molecules would have a negligible effect on the results of the calculations. The starting structures for the eight solute/solvent models (Figure 2) were equilibrated for a time period of no less than 250 ps to allow for relaxation and reorientation of the solvent molecules around the solute. These equilibrated structures were used as starting points ($\lambda = 1$) for each of the seven model systems used in the FEP simulations.

Experimental Protocol

The MD simulations were carried out using a modified parallel version of the SANDER module from AMBER4.1[75] running on the Cray-T3D at the Pittsburgh Supercomputing Center. The system was held at 300 K and 1 atm using the Nosé−Hoover Chain constant temperature and pressure algorithms utilizing periodic boundary conditions.[76] The simulations were completed using a 1.5 fs time step in conjunction with the SHAKE algorithm to constrain all bonds.[77,78] A nonbond cut-off distance of 10 Å was used, and the nonbond pair list was updated every 20 steps. The 1−4 van der Waals and electrostatic interactions were scaled by 1/7.4 and 1/1.2, respectively.[16,79] The solvent box was initially equilibrated for 900 ps and sampled for an additional 450 ps with atomic coordinates being collected every 40 steps. The partial atomic charges for the solutes were obtained with quantum mechanical electrostatic potential (ESP) fitting using the 6-31G* basis set.[80−82] Once the fitting was completed, the atomic charges on equivalent hydrogen atoms were symmetrized.

The OPLS[64] united atom AMBER force field[70] was used to model octanol and the solutes, while the saturating water molecules were TIP3P.[65] The all-atom OPLS parameters for benzene and phenol were those of Jorgensen.[71−74] Ethylbenzene was treated as a hybrid with the methyl and methylene groups treated as united atoms and the remaining carbon and hydrogen atoms treated as all-atoms which is analogous to Jorgensen's all-atom OPLS model for toluene.[72,83]

Free energy perturbation calculations were carried out in which a series of seven small organic solutes (see Figure 2) were gradually mutated into seven different structures as shown

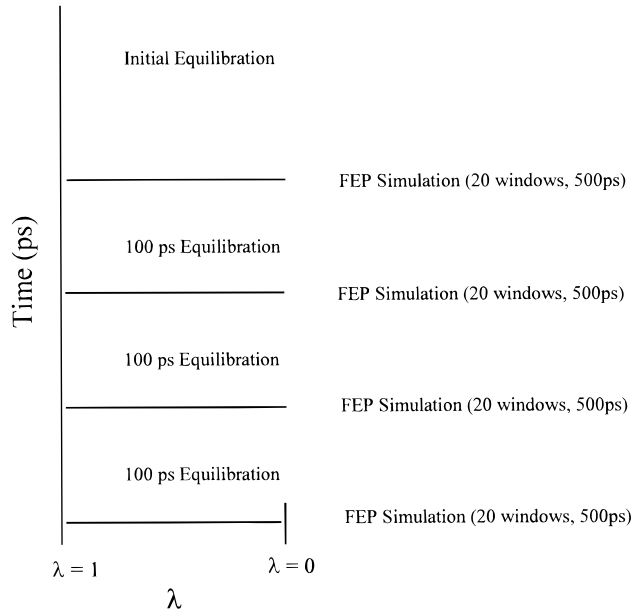

Figure 3. Schematic illustration of the procedure carried out for each FEP simulation. This protocol allows us to estimate the error associated with each perturbation.

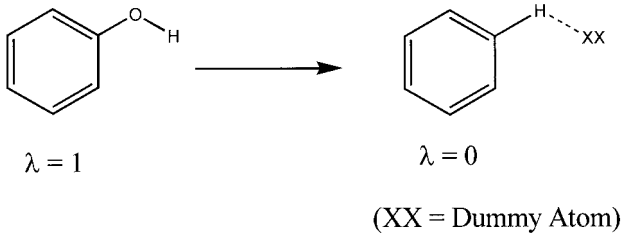

Figure 4. Mutation of phenol into benzene for the FEP simulations in water and water- saturated octanol.

in Figure 3. Each mutation involved no more than two atoms in order to simplify the calculation. For example, in the phenol-to-benzene perturbation, the phenol oxygen is mutated into a benzene hydrogen atom, and the hydroxyl hydrogen of phenol is mutated into a dummy atom (Figure 4). The bonded parameters for dummy atoms were chosen to be identical to the corresponding "real" atom parameters. The dummy atoms were also given a zero well depth, as well as no charge in order to eliminate their contribution to the free energy. Each of these seven perturbations was carried out in both aqueous and water-saturated octanol solutions.

The FEP simulations were carried out using the AMBER4.1 suite of programs.[84] The starting configurations for each simulation were initially equilibrated for 250 ps prior to running the perturbation calculations. The simulations were carried out at constant temperature (300 K) and pressure (1 atm), utilizing separate temperature coupling for the solute and solvent.[85] Periodic boundary conditions were utilized and a 1.5 fs time step was used for the simulation. All bonds within the system were constrained to their equilibrium distances using the SHAKE algorithm in order to remove the high-frequency motions.[77,78] The nonbond cut-off distance was 10 Å, and the nonbond pair list was updated every 20 steps. All intramolecular perturbed group energies were included in the calculation of the free energy change.

Each simulation utilized the thermodynamic integration (TI) FEP technique[69] as implemented in AMBER 4.1. The simulations were carried out in one direction from $\lambda = 1$ to $\lambda = 0$ (a lambda value of 1 represents the initial state, and a lambda value of 0 represents the final perturbed state). All of the perturbations were run for a total of 500 ps except for the acetamide-to-acetone perturbation which was run for a total of 1 ns. The perturbations were run over 20 windows with 10 ps of equilibration and 15 ps of sampling at each window.

In order to assess the reproducibility of each perturbation, four separate FEP calculations were completed for each of the seven different models as shown in Figure 2. A scheme illustrating this methodology is illustrated in Figure 3. After an initial equilibration period, the first FEP simulation is run. The starting point of the first FEP simulation is then equilibrated for an additional 100 ps so as to provide a new starting point for the second FEP simulation. This FEP simulation is identical to the first, other than for the additional equilibration period. This process is repeated two additional times and provides an estimate of the precision associated with each model. This procedure was adopted for both the aqueous FEP simulations as well as for those in water-saturated octanol. A total of 56 FEP simulations were performed for the seven perturbations illustrated in Figure 2 (four for each model in both water and water-saturated one-octanol).

A simple procedure was followed for the GB/SA calculations in water and octanol. Each solute was minimized in either GB/SA water[86] or octanol, and the corresponding free energies of solvation were determined. These ΔG_{oct} were then used to calculate log P_{ow} and Δlog P_{ow} values for comparison with the FEP simulations. Analogous to the FEP simulations, only the GB/SA solvation free energies were considered. This assumes that the change in the solute internal free energy in going from octanol to water is negligible. For the small solutes in this study, that assumption is probably reasonable. However, we have seen examples,[87] particularly with large floppy solutes, where this assumption is not valid.

Physical Properties of the Equilibrated Octanol/Water Box

The water-saturated octanol model that was adopted for this study was based on a modification[16] of Jorgensen's united atom OPLS parameters for alcohols.[73] In order to accurately predict solvation free energies, the systems studied required extensive equilibration because the solvent molecules were initially arranged in random configurations throughout the solvent box. During this equilibration period, both water and octanol solvent molecules were able to diffuse freely throughout the solvent box. In the past, this high computational expense has been the primary reason that octanol has not been studied as a solvent since sufficient sampling of phase space has traditionally been a problem. The development of parallel computing has made longer simulation times more feasible and have allowed for systems of this nature to be thoroughly examined.

Once the box was sufficiently equilibrated, a number of physical quantities were calculated in order to compare the results of this simulation to experiment. The system density and self-diffusion coefficients were calculated for both water and water-saturated octanol and compared to experiment. The structure of the solvent mixture was also examined through visual inspection (e.g., see Figure 1) and the calculation of radial distribution functions.[88]

Volume of the Solvent Mixture

The experimental volume of the water-saturated octanol binary solvent mixture can be estimated using the experimental volume per molecule for octanol (262.8 Å^3) and water (29.76 Å^3).[89] The solvent mixture in this study contains 125 octanol

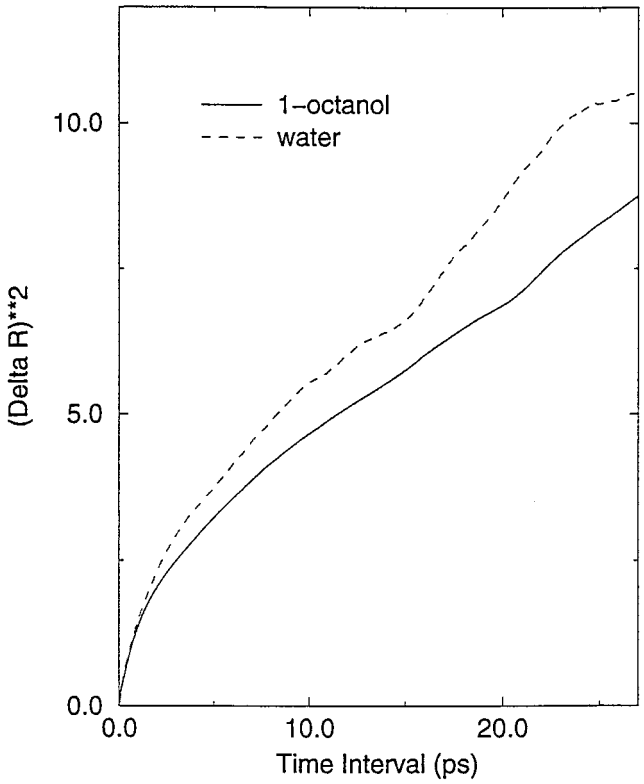

Figure 5. Plot of $r_i(\Delta t)^2$ versus time interval Δt. The upper curve (dashed line) corresponds to the diffusion of water molecules, and the lower curve (solid line) pertains to the diffusion of octanol molecules for the simulations which were run at 27 °C.

and 42 water molecules which corresponds to an estimated experimental volume of 34 100 Å^3/system. The octanol/water volume calculated in our simulation is 33 700 ± 181 Å^3/system, which compares favorably to a previously calculated value (34 014 ± 402 Å^3/system[16]) and the estimated experimental value.

Self-Diffusion Coefficients

Self-diffusion coefficients were calculated for both octanol and water in the solvent mixture. The self-diffusion coefficients were computed from a plot of $(r_i(\Delta t))^2$ versus the time interval Δt as shown in Figure 5. The plot was generated from the final 60 ps of the simulation. The upper curve corresponds to the diffusion of the water molecules, and the lower curve represents the diffusion of the octanol molecules. The self-diffusion coefficients were computed to be 0.55×10^{-5} and 0.42×10^{-5} cm^2/s for water and octanol, respectively, at 27 °C. The experimental value for neat octanol was determined to be 0.18×10^{-5} cm^2/s at 25 °C.[90] The experimental self-diffusion coefficient for pure water at 25 °C is 2.30×10^{-5} cm^2/s.[91] The computed octanol self-diffusion coefficient indicates that the presence of water may be responsible for slightly increasing the ability of octanol molecules to diffuse within the solvent box. On the contrary, the diffusion coefficient for water is considerably smaller than seen experimentally in pure water. This is not surprising since the long hydrocarbon chains of octanol solvent molecules form large hydrophobic regions within the box and restrict the flow of the water molecules. These results exhibit the same trends as those computed previously.[16]

Structure of Water-Saturated 1-Octanol

The internal structure of water-saturated octanol was examined through visual inspection as well as through radial

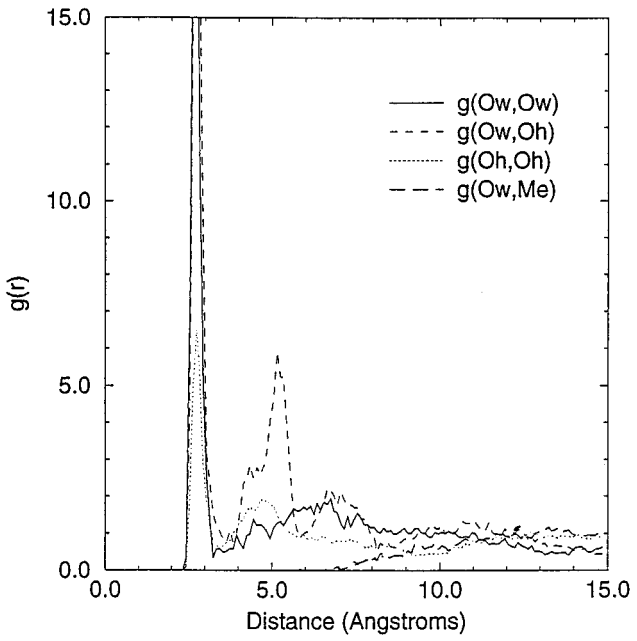

Figure 6. Radial distribution functions for water-saturated octanol. Plots are *g*(Ow,Ow) (solid line) between water oxygen atoms, *g*(Ow,Oh) (dashed line) between water oxygen and octanol oxygen, *g*(Oh,Oh) (dotted line) between octanol oxygen atoms, and *g*(Ow,Me) (long dashes) between water oxygen and octanol terminal methyl groups.

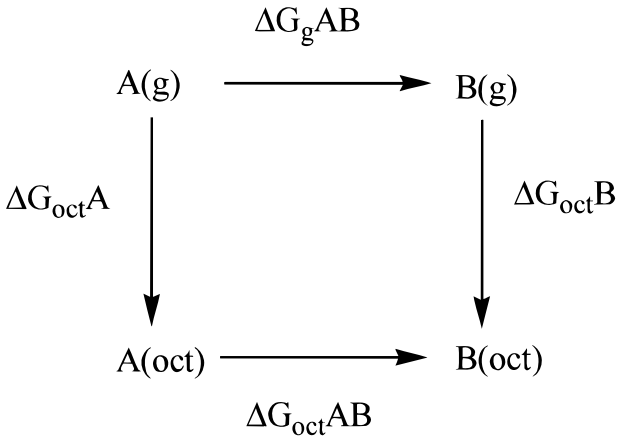

Figure 7. Thermodynamic cycle for calculating relative free energies of solvation.

distribution functions (RDFs).[88] As expected, there is extensive hydrogen bonding throughout the solvent mixture as evidenced in Figure 1. In this illustration, the oxygen atoms of both octanol and water are represented by van der Waals surfaces and the hydrocarbon tails are shown as solid lines. This behavior is quite common in liquid solvents such as alcohols or other solvents which have polar and nonpolar regions.[90,92−96] Hydrogen-bonded clusters of varying sizes are distributed throughout the solvent mixture which lead to the creation of local polar regions (Figure 1). The hydrophobic tails also tend to associate with one another as clearly visible in Figure 1. We also find that the water molecules preferentially coordinate to other water molecules rather than to the octanol hydroxyl head groups.

RDFs provide a means by which the local environment of either a water or octanol solvent molecule can be studied (see Figure 6). This plot shows similar trends when compared to the previously calculated RDF plot.[16] The three oxygen RDFs, *g*(Ow,Ow) (solid line), *g*(Ow,Oh) (dashed line), and *g*(Oh,Oh) (dotted line) of Figure 6 reveal a highly structured polar region in the octanol/water mixture. The first peak for *g*(Ow,Ow) is

TABLE 1: FEP Results for Calculating Free Energies of Solvation in Water-Saturated Octanol (kcal/mol)

perturbation	$\Delta\Delta G_{oct}{}^1$	$\Delta\Delta G_{oct}{}^2$	$\Delta\Delta G_{oct}{}^3$	$\Delta\Delta G_{oct}{}^4$	average	experiment[a]	error
ethylbenzene − phenol	−4.52	−4.87	−3.57	−5.38	−4.58 ± 0.76	−3.51	−1.07
cyclopentane − tetrahydrofuran	−0.61	−0.69	−0.37	−0.68	−0.58 ± 0.14	−1.23	0.65
isopropanol − isobutane	3.60	4.10	4.83	5.22	4.45 ± 0.71	3.39	1.06
phenol − benzene[b]	4.55	4.22	4.27	4.46	4.38 ± 0.15	4.79	−0.41
pyridine − benzene	−0.75	−0.77	−1.11	−0.83	−0.87 ± 0.18	1.79	−2.66
methylamine − methanol	−0.51	−0.13	−0.01	−0.21	−0.22 ± 0.21	−0.25	0.03
acetamide − acetone (shorter sim.)[c]	5.10	6.09	7.46	9.19	6.96 ± 0.89	4.42	2.54
acetamide − acetone (longer sim.)[d]	7.81	8.02	8.18	7.85	7.97 ± 0.10	4.42	3.55
average unsigned error[e]							1.34

[a] Experimental free energies of solvation for water-saturated octanol were obtained through back-calculating these values using eq 1 given experimental log P_{ow} values[3] and aqueous free energies of solvation.[103−106] [b] DeBolt and Kollman computed the free energy of solvation to be 3.80 ± 0.35 kcal/mol.[16] [c] Simulation was run for a total of 500 ps. [d] Simulation was run for 1 ns in order to obtain converged free energy values. [e] Calculated using the error from the longer acetamide−acetone simulation; the shorter simulation gives a smaller error.

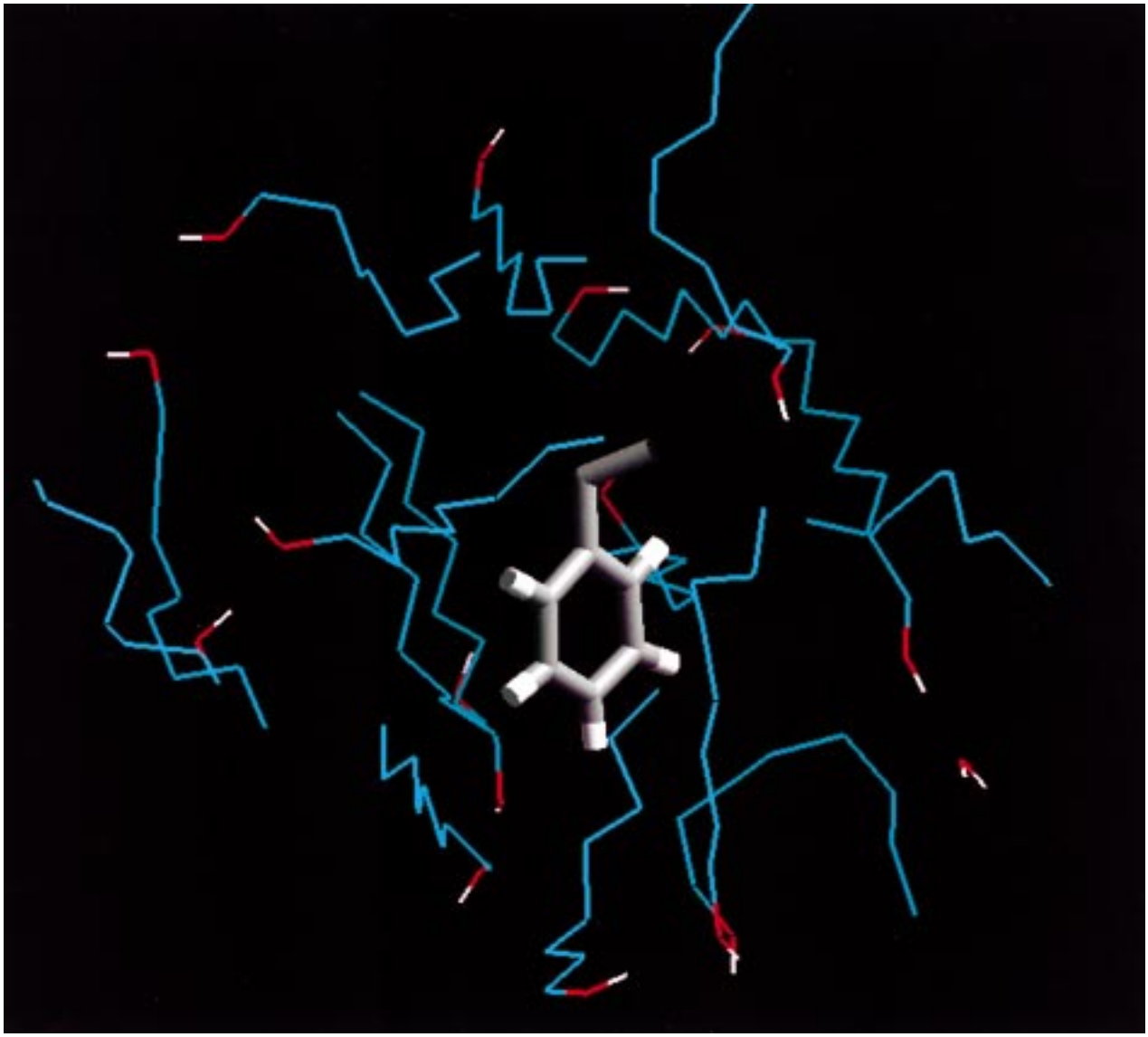

Figure 8. View of ethylbenzene within a 8.0 Å solvation shell of water-saturated octanol.

quite intense at a distance of 2.7 Å. This is in support of Figure 1 indicating there is a high probability of finding waters which are in the vicinity of other water molecules in the solvent mixture. It also indicates that the majority of water molecules are located closer to the center of the inverted-micellar regions. The *g*(Ow,Me) curve indicates that the water oxygen atoms and the terminal methyl groups of octanol are spatially separated and have very weak interactions as expected. The polar region in this study was computed to be slightly larger than the polar region in the previous simulation of water-saturated octanol (11.5 Å as compared to 9.5 Å).[16]

In summary, the results of the analyses performed on this model system are in good agreement with experimental results as well as with prior theoretical results on a similar water-saturated octanol solvent model.[16] We note that the main difference between our MD study and the previous one has to do with the use of a better *T* and *P* coupling scheme (Berendsen[85] scheme versus Nose−Hoover Chain method[76]).

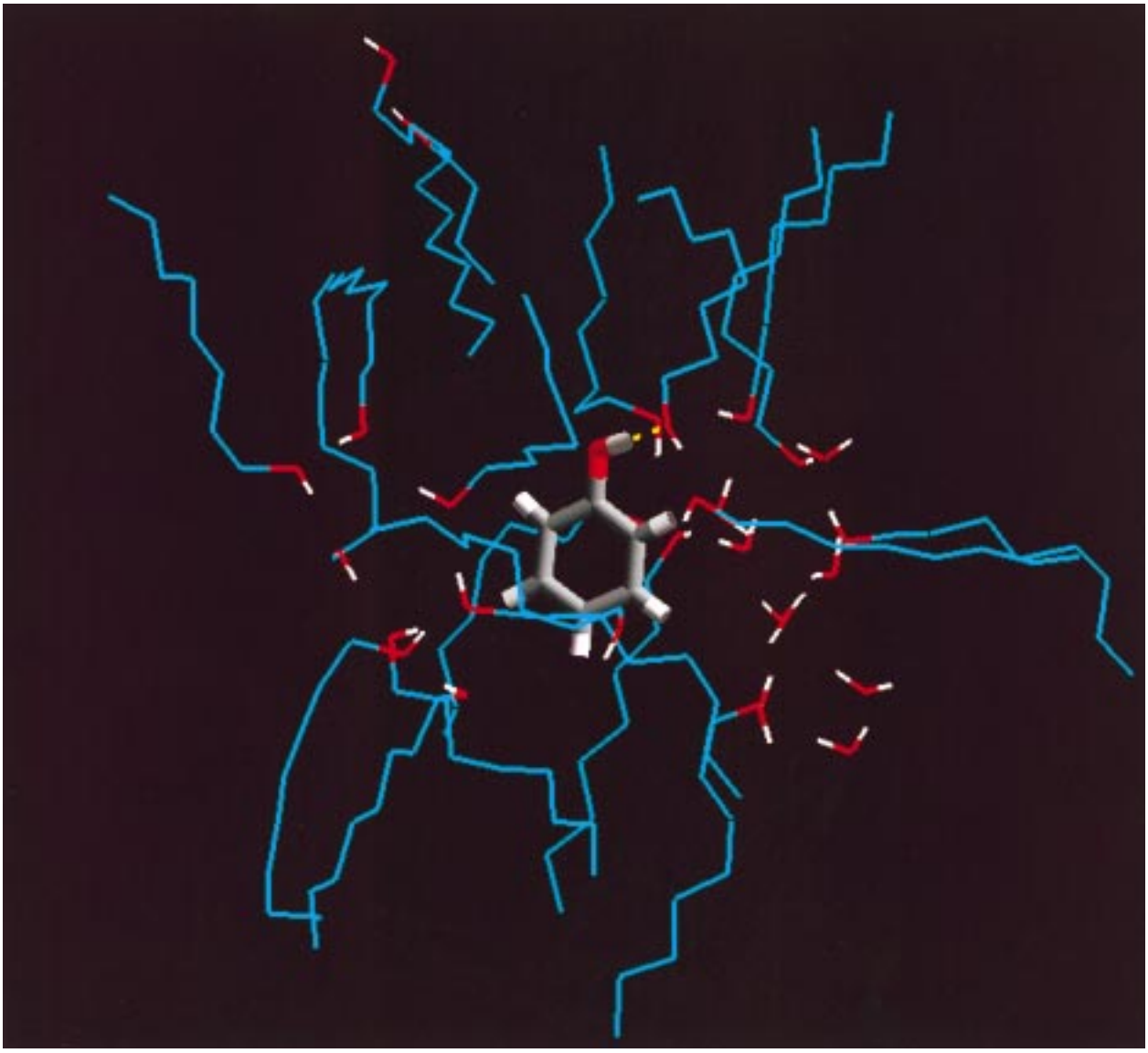

Figure 9. View of phenol within a 8.0 Å solvation shell of water-saturated octanol.

We also employed TIP3P instead of SPC waters in both the water and water-saturated octanol simulations. Based on the solution properties described above, it appears that this should be a good model for studying the dynamics as well as the solvation of small organic molecules in a water-saturated octanol−solvent mixture.

Free Energies of Solvation for Water-Saturated Octanol

The previous description of the internal structure of the solvent model illustrates the reason why this solvent mixture is ideally suited for modeling membranes and predicting the lipophilicity of molecules. There are essentially two phases which are present in this solvent model as both polar and hydrophobic regions are located throughout the solvent mixture. The amphiphilic nature of the solvent structure enables a solute to partition itself into a polar region, a hydrophobic region, or into the hydrophobic−hydrophilic interface. The location of the solute is entirely dependent on the nature of the solute. As an example, a highly polar molecule would most likely reside in a polar region while an amphipathic solute would be located near the interface of the hydrophobic and hydrophilic regions.

MD-FEP simulations were carried out on a series of small organic solutes in order to observe the partitioning phenomena and to predict a relative octanol/water partition coefficient for each model system that is shown in Figure 2. The octanol/water partition coefficients were computed from the free energies of solvation for the solutes in both water and in the water-saturated octanol−solvent mixture. There have been previous studies in which FEP investigations were run in organic solvents other than octanol such as carbon tetrachloride[49,50] and chloroform.[51−56] There has been only one study to date which has used water-saturated octanol as the solvent model and it examined only a single permutation involving two solutes, the conversion of phenol into benzene.[16,97] In order to better assess FEP for calculating the log P_{ow} of organic solutes, we examined seven permutations that involve 12 different solutes.

FEP simulations have been extensively utilized as a method for calculating free energies of solvation, ΔG_{Sol}, for a wide range of solutes.[10,66−69,98] The thermodynamic cycle used for calculating free energies of solvation is depicted in Figure 7. In computing the solvation free energies in this study, it was assumed that there were comparable internal contributions to the free energies in the gas phase and in solution. Therefore, ΔG_gAB can be neglected and the relative solvation free energy $\Delta\Delta G_{oct}$, was determined by a FEP calculation of ΔG_{oct}AB.[53,99]

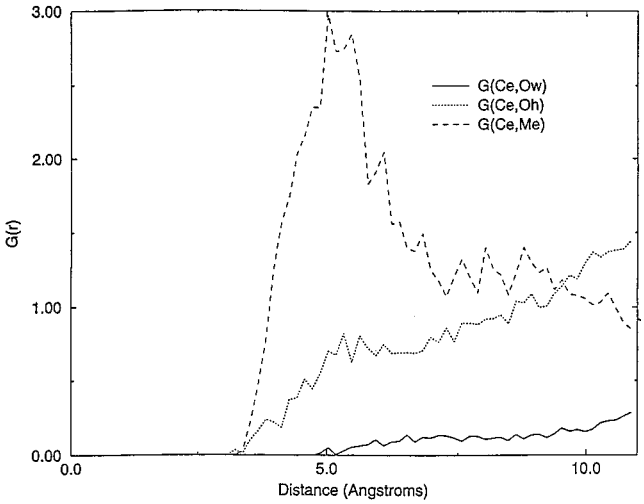

Figure 10. RDFs for ethylbenzene in water-saturated octanol obtained from a 100 ps trajectory at the beginning of the FEP simulation. In this coordination plot, the ethylbenzene carbon atom α to the aromatic ring (Ce) is central (R = 0). Represented are the interactions between ethylbenzene and (1) saturating water molecules, *g*(Ce,Ow) (solid line), (2) octanol oxygen atoms, *g*(Ce,Oh) (dotted line), (3) octanol methyl groups, *g*(Ce,Me) (dashed line).

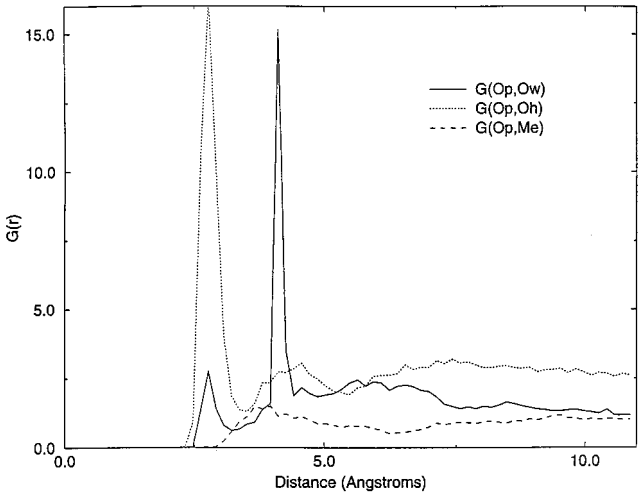

Figure 11. RDFs for phenol in water-saturated octanol obtained from a 100 ps trajectory at the beginning of the FEP simulation. In this coordination plot, the phenol oxygen (Op) is central (R = 0). The interactions are between benzene and (1) saturating water molecules, *g*(Op,Ow) (solid line), (2) octanol oxygen atoms, *g*(Op,Oh) (dotted line), (3) octanol methyl groups, *g*(Op,Me) (dashed line).

The results of the FEP calculations for water-saturated octanol are shown in Table 1. Average free energies of solvation were calculated from the four separate FEP simulations that were completed for each model system as shown in Figure 3. The uncertainty for each perturbation is also included and is expressed as the estimated deviation of the mean, $\pm 1\sigma_m$. The experimental relative free energies of solvation for each FEP carried out (see Figure 2) are also given in Table 1.

Obtaining experimental free energies of solvation for this solvent mixture is not straightforward. There have been a limited number of studies concerning the experimental determination of ΔG_{oct} in the literature. Most of the studies have examined the solvation free energy for transferring a small solute from neat octanol to water-saturated octanol.[100−102] Fortunately, a very large number of experimental log P_{ow} values are available.[3] These were combined with experimentally determined free energies of solvation in water[103−106] to back-calculate the free energy of solvation for the solvent mixture. In using this method to compute ΔG_{oct}, additional uncertainty is introduced since the value is computed as a difference of two experimental quantities. However, these back-calculated values for log P_{ow} should still provide a reasonable estimate of the free energy of solvation for water-saturated octanol.

TABLE 2: Hydrogen Bonding between Phenol and either Water or Octanol Solvent Molecules for the Phenol-to-Benzene FEP Simulation[a]

hydrogen donor	hydrogen acceptor	frequency[b] (%)
octanol	phenol	57.8
water	phenol	2.3
phenol	octanol	74.8
phenol	water	21.8

[a] Data was obtained from a 100 ps trajectory generated at the end point of the simulation. [b] Represents the percentage of the time a hydrogen bond was present during the 100 ps trajectory.

The calculated and experimental changes in solvation free energies are in generally good agreement, demonstrating that it is practical to calculate free energies of solvation even in a complex solvent mixture such as water-saturated octanol. The differences between the computed and experimental free energies of solvation in water-saturated octanol are typically less than 1.1 kcal/mol, except for the acetamide-to-acetone and pyridine-to-benzene perturbations that had errors in excess of 2.5 kcal/mol. It should be kept in mind that in this case the experimental ΔG_{oct} values have been estimated from the difference in experimental log P_{ow} and ΔG_{aq} data, and are expected to have larger uncertainties associated with them due to additivity of errors. Nevertheless, the errors in the acetamide−acetone simulations in water-saturated octanol are far too large to explain away as propagation of errors in the experimental data.

Examination of the Solute Environment in Water-Saturated Octanol

The location of the solute in the solvent mixture is entirely dependent on the nature of the solute. A polar solute would be expected to migrate and reside in or near the polar core of an inverted-micellar region. In contrast, a hydrophobic solute would most likely be found in the hydrophobic tail regions of octanol. During MD equilibration, some solvent reorientation would be expected in order to promote favorable interactions between the solute and solvent. In order to determine if the solvent model in this study was capable of the selective migration of the solutes to a preferential location in the solvent mixture, individual snapshots of both the starting structures ($\lambda = 1$) and the ending structures ($\lambda = 0$) for the seven FEP simulations were generated. Visual inspections of these snapshots and analyses of 100 ps MD trajectories at the beginning ($\lambda = 1$) and end ($\lambda = 0$) of the FEP simulations illustrate the partitioning of the various solutes within the solvent mixture. Only two of the FEP simulations will be discussed in detail, but these are representative of the other simulations.

Solute Environments

In order to gain further insight into the solute's local environment, MD simulations (100 ps) were performed at both the beginning and end point of each FEP simulation. The first simulation that was examined in detail was the gradual mutation of ethylbenzene into phenol. Individual snapshots of the starting (ethylbenzene) and end points (phenol) of the FEP simulation are shown in Figures 8 and 9. Ethylbenzene is a relatively

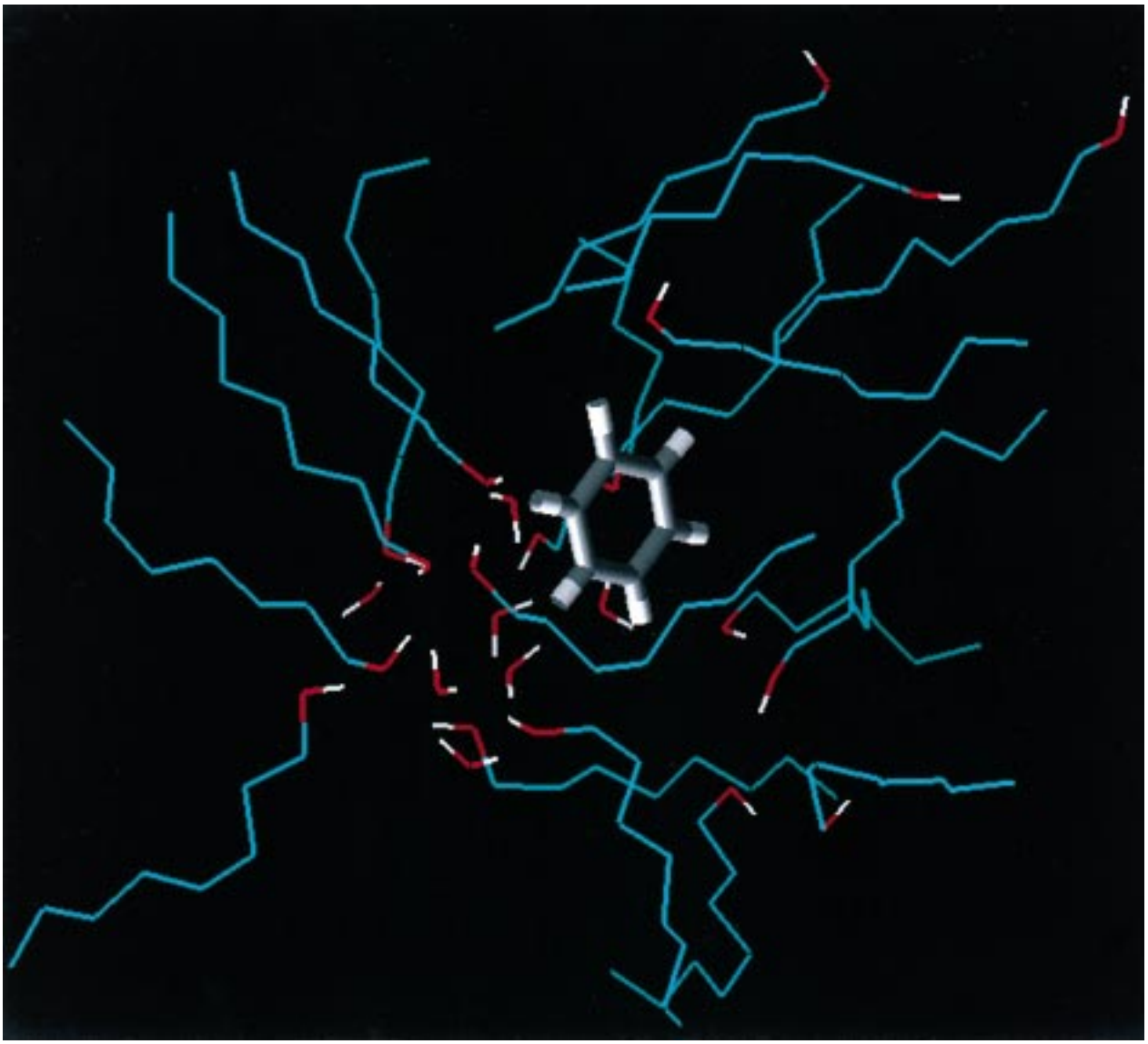

Figure 12. View of benzene within a 8.0 Å solvation shell of water-saturated octanol.

nonpolar solute and would be expected to preferentially reside in a region composed of the hydrocarbon tails of octanol. Figure 8 indicates this is the case since the solute is located entirely in a hydrophobic region. Three solute−solvent RDFs for ethylbenzene in water-saturated octanol are shown in Figure 10. The central atom (R = O) in these plots is the carbon atom α to the aromatic ring. These RDFs clearly indicate that ethylbenzene resides in the hydrophobic region of the solvent system. There are no water molecules in the vicinity of the solute, nor are there any polar head groups of octanol oriented toward the solute.

During the FEP simulation, ethylbenzene is slowly mutated into the more polar molecule, phenol. The environment around phenol is much different than that seen with ethylbenzene as shown in Figure 9. Phenol resides in a polar region where water molecules have diffused into the region around the solvent and the octanol molecules have reoriented themselves.

Next we examined the FEP simulation involving the mutation of phenol into benzene. The starting structure for this simulation resembles the previously described (Figure 9) structural environment for phenol in which the solute is located in the inverted-micellar region. The RDFs for this model system (which are of relevance to the ethylbenzene-to-phenol case discussed above) are shown in Figure 11. This plot illustrates the preference of phenol to reside in a polar region of the solvent mixture. A hydrogen bond analysis was completed to determine if hydrogen bonding was present between phenol and the solvent. The results of the analysis are shown in Table 2 and they illustrate the presence of an extensive hydrogen bonded network in which phenolic oxygen atoms act both as a hydrogen bond donor and acceptor.

Benzene is less hydrophilic and, not unexpectedly, resides in a more hydrophobic region as shown in Figure 12. The RDFs for benzene are based on a benzene hydrogen atom serving as the central atom (R = 0) in place of the phenol oxygen atom (Figure 13). The interaction between benzene and the water molecules is interesting because of the presence of a water/benzene π-complex (see peak at 4.5 Å in Figure 13). This intermolecular interaction has been observed before and can be attributed to the dipole momement of the water molecules interacting with the quadrupole moment of the benzene ring.[107−110]

Calculation of Octanol/Water Partition Coefficients

In order to compute octanol/water partition coefficients (log P_{ow}) directly, the free energies of solvation must be calculated in both aqueous and organic phases. Given the appropriate free energies of solvation, computation of the partition coefficient

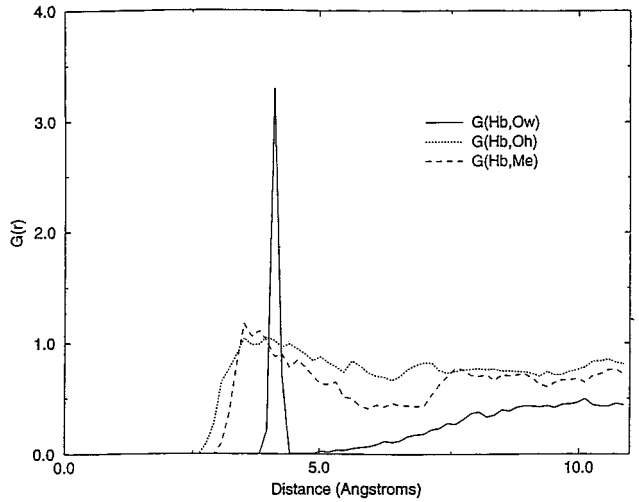

Figure 13. RDFs for benzene in water-saturated octanol obtained from a 100 ps trajectory at the end point of the FEP simulation. In this coordination plot, the benzene hydrogen atom (Hb) is central (R = 0). The interactions represented are between benzene and (1) saturating water molecules, *g*(Hb,Ow) (solid line), (2) octanol oxygen atoms, *g*(Hb,Oh) (dotted line), (3) octanol methyl groups, *g*(Hb,Me) (dashed line).

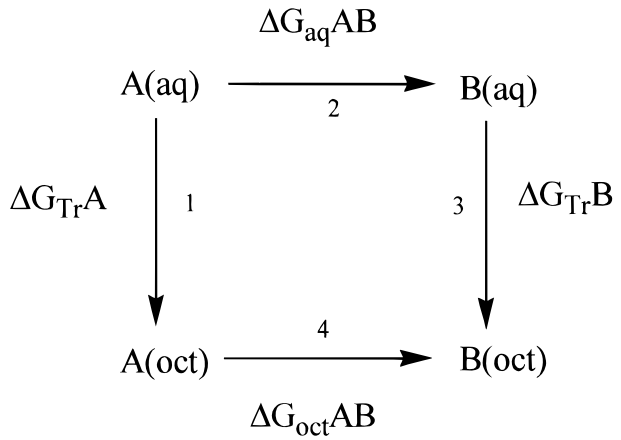

Figure 14. Thermodynamic cycle that was utilized in the calculation of octanol/water partition coefficients.

becomes straightforward. For example, consider solute A. Initially, the free energies of solvation are determined in the aqueous phase, ΔG_{aq}A, and in the water-saturated octanol phase, ΔG_{oct}A . The difference between the solvation free energies is the free energy of transfer (ΔG_{Tr}A) for transferring solute A from water to water-saturated octanol. This process is illustrated for two different solutes A and B by the vertical paths 1 and 3 in Figure 14. The free energy of transfer for solutes A and B is related to octanol/water partition coefficients for A (log P_{ow} (A)) and B (log P_{ow} (B)) through eqs 1 and 2, respectively, where R is the gas constant and T is the temperature:

$$\Delta G_{Tr}\mathrm{A} = -230RT \log P_{ow}\,(\mathrm{A}) \qquad (1)$$

$$\Delta G_{Tr}\mathrm{B} = -230RT \log P_{ow}\,(\mathrm{B}) \qquad (2)$$

Equations 1 and 2 can be used to compute log P_{ow} values if absolute free energies of solvation can be calculated using, for example, the GB/SA continuum solvation model.[62,63] Unfortunately, it is difficult to compute absolute free energies of solvation using FEP simulations.[16] It is, however, computationally feasible to calculate a relative free energy of solvation in which solute A is slowly mutated into solute B. Thus, by taking advantage of the fact that free energy is a state function, the following relationship can be utilized based on the free energy cycle given in Figure 14:

$$\Delta G_{oct}\mathrm{AB} - \Delta G_{aq}\mathrm{AB} = \Delta G_{Tr}\mathrm{B} - \Delta G_{Tr}\mathrm{A} = \Delta\Delta G_{Tr}\mathrm{AB} \qquad (3)$$

The relative free energies of solvation of A and B can be used to calculate a relative free energy of transfer $\Delta\Delta G_{Tr}$AB. This allows the relative partition coefficient (Δlog P_{ow}) for solutes A and B to be calculated from the direct relationship between $\Delta\Delta G_{Tr}$AB and Δlog P_{ow} as illustrated in eq 4:

$$\Delta\Delta G_{Tr}\mathrm{AB} = -2.30RT\Delta \log P_{ow} \qquad (4)$$

Free energies of solvation for water were calculated utilizing the same protocol that was described in the calculation of the free energies of solvation in the water- saturated octanol−solvent mixture. The results of these calculations are shown in Table 3. For the water simulations, the acetamide-to-acetone perturbation was much less problematic than was the case in water-saturated octanol. In water, this perturbation showed good consistence between runs and gave results that are in excellent agreement with experiment. However, the errors associated with the other nitrogen-containing compounds were much larger in water, as were the errors in simulations involving phenol. Difficulties with nitrogen-containing solutes in water have been observed before, and this error has been variously ascribed to neglect of polarization, charge transfer, or conformational effects.[99,111−114]

Relative partition coefficients were computed from eq 4 using the average solvation free energies in water and water-saturated octanol.[115] The computed Δlog P_{ow} values along with a comparison to experimental results are given in Table 4. Positive values of Δlog P_{ow} indicate that the change from A to B results in an increased affinity for the water-saturated octanol over pure water.[52] Experimental values for Δlog P_{ow} were obtained from the differences in the absolute log P_{ow} values for each solute.[3]

The FEP calculated partition coefficients are in good agreement with experiment giving an average unsigned error of about 1 log unit. This error would be much smaller (0.74 log unit) if the acetamide−acetone perturbation, which has a large systematic error in the FEP simulations, was not included. In an earlier study,[16,97] benzene was mutated into phenol and a Δlog P_{ow} of −0.76 was computed. In this study we examined the reverse perturbation of phenol to benzene and obtained a Δlog P_{ow} of −0.45 as compared to an experimental Δlog P_{ow} of 0.67.[3] The largest error in Δlog P_{ow} in this study is found for the perturbation of acetamide to acetone. The error in Δlog P_{ow} for this perturbation is more than 2.5 log units. The large error in the FEP calculated Δlog P_{ow} for acetamide−acetone is a direct result of a calculated change in the free energy of solvation in water-saturated octanol that is much too positive. Longer simulations in water-saturated octanol were better converged, but the ΔG_{oct} was still in very poor agreement with experiment. Presumably, this is due to limitations in the classical representation we employed. Nevertheless, considering the complexity of the water-saturated octanol−solvent mixture, the good results obtained from the other six perturbations are encouraging.

The Δlog P_{ow} values were also compared to those calculated utilizing the GB/SA continuum solvent model.[13,14,62] Absolute solvation free energies were calculated for each solute utilizing the GB/SA octanol model[62] and the Merck Molecular Force Field (MMFF)[117] as implemented in MacroModel 5.5.[118] The computed octanol and water[86] free energies of solvation were combined to calculate the partition coefficient for each solute

TABLE 3: FEP Results for Calculating Free Energies of Solvation in Water (kcal/mol)

perturbation	$\Delta\Delta G_{aq}^1$	$\Delta\Delta G_{aq}^2$	$\Delta\Delta G_{aq}^3$	$\Delta\Delta G_{aq}^4$	average	experiment[a]	error
ethylbenzene − phenol	−7.65	−7.00	−7.30	−7.51	−7.37 ± 0.14	−5.80	−1.57
cyclopentane − tetrahydrofuran	−3.76	−3.97	−3.86	−3.69	−3.82 ± 0.12	−4.71	0.89
isopropanol − isobutane	6.35	5.85	6.87	6.66	6.43 ± 0.44	7.10	−0.67
phenol − benzene[b,c]	3.75	3.67	3.86	3.74	3.76 ± 0.08	5.70	−1.94
pyridine − benzene	1.55	1.50	1.70	1.53	1.57 ± 0.09	3.80	−2.23
methylamine − methanol[d]	−2.28	−2.16	−2.24	−2.03	−2.18 ± 0.11	−0.60	−1.58
acetamide − acetone	5.67	5.72	5.69	5.70	5.70 ± 0.02	5.81	−0.11
average unsigned error							1.28

[a] Experimental aqueous free energies obtained from references 103−106. [b] Jorgensen and Nguyen computed a hydration energy of 5.2 ± 0.2 kcal/mol in TIP4P water.[83] [c] DeBolt and Kollman computed a hydration energy of 4.89 ± 0.20 kcal/mol in SPC water.[16] [d] Nagy et al. computed a hydration energy of −2.0 kcal/mol.[116]

TABLE 4: Comparison of Methods for Calculating Octanol/Water Partition Coefficients

perturbation	experimental[a] $\Delta\log P$	$\Delta\log P$ (FEP)	error	$\Delta\log P$ (GB/SA)	error
Ethylbenzene − Phenol	−1.69	−2.05	−0.36	−0.95	0.74
Cyclopentane − Tetrahydrofuran	−2.54	−2.38	0.16	−2.31	0.23
Isopropanol − Isobutane	2.71	1.45	−1.26	2.17	−0.54
Phenol − Benzene[b]	0.67	−0.45	−1.12	0.77	0.10
Pyridine − Benzene	1.48	1.79	0.31	1.50	0.02
Methylamine − Methanol	−0.20	−1.44	−1.24	1.37	1.57
Acetamide − Acetone[c]	1.02	−1.66	−2.68	0.73	−0.29
average unsigned error			1.01		0.50
			0.74[d]		

[a] Experimental log P_{ow} values were obtained from Hansch and Leo.[3] [b] DeBolt and Kollman computed $\Delta\log P_{ow} = 0.76$.[16] [c] $\Delta\log P_{ow}$ calculated from the longer FEP simulation. [d] Omitting the acetamide−acetone perturbation.

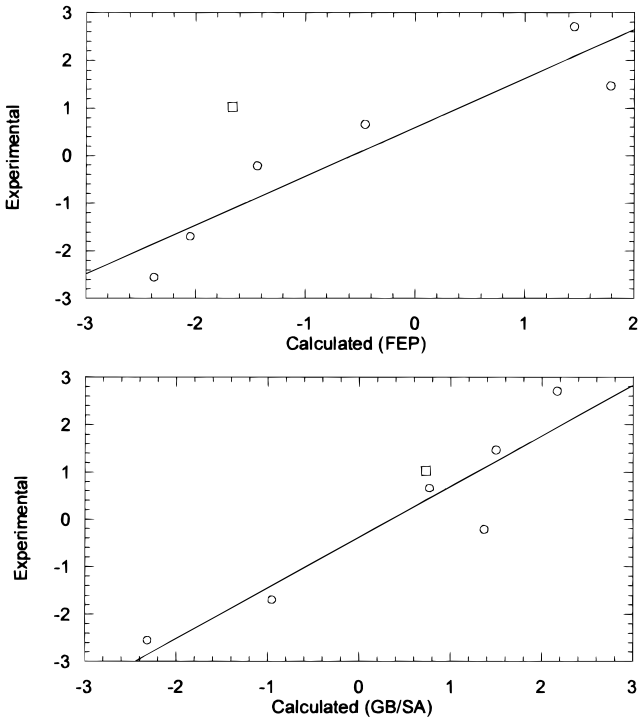

Figure 15. Comparison of experimental $\Delta\log P$ values to (a) computed $\Delta\log P$ values calculated using FEP methodology ($r^2 = 0.87$ neglecting acetamide−acetone datapoint; shown as open square) and (b) computed $\Delta\log P$ values calculated using the GB/SA model ($r^2 = 0.86$ including acetamide−acetone).

using eq 4. Relative partition coefficients were calculated from the differences in the absolute values. The computed $\Delta\log P_{ow}$ values using the GB/SA model are reported in Table 4, and give an average unsigned error of 0.50 log units. Plots comparing the experimental and FEP or GB/SA calculated $\Delta\log P_{ow}$ values are given in Figure 15. The calculated and observed $\Delta\log P_{ow}$ values show a strong correlation with $r^2 = 0.87$ for both the FEP and GB/SA simulations, respectively, if the FEP results for acetamide−acetone are omitted. If one includes the acetamide−acetone perturbation, then the r^2 for the FEP calculations falls to 0.69. Interestingly, the GB/SA calculations give results that are superior to the much more expensive FEP simulations, particularly if one includes the FEP results for the acetamide−acetone perturbation.

The FEP simulations do have an advantage over the GB/SA method that goes beyond comparison of the accuracy of $\Delta\log P_{ow}$. Because solvent molecules are included explicitly, the FEP simulations can provide molecular-level details and insights that cannot be obtained using a continuum solvent model. For example, solute−solvent interactions such as hydrogen bond formation may play an important role in the design of an enzyme inhibitor. This type of detailed solvent structure is unavailable in a continuum method. The principal advantage of the GB/SA model is its computational efficiency. This makes it much better suited for applications such as QSAR where a large number of log P_{ow} values need to be evaluated. For example, the calculation of a $\Delta\log P_{ow}$ may take minutes with the GB/SA model while the FEP approach may take days of CPU time. Hence, the method of choice (FEP versus GB/SA) depends on the type of problem one wants to solve.

Conclusions

FEP calculations were carried out for a series of small organic molecules in a box of water-saturated octanol in order to gain insight into the structural characteristics of both the solute and solvent molecules. Both aqueous and water-saturated octanol free energies of solvation were determined in order to calculate relative partition coefficients for each perturbation. Results of the FEP calculations were in generally good agreement with experimental relative partition coefficients, $\Delta\log P_{ow}$, except for the acetamide−acetone perturbation that gave an error in $\Delta\log P_{ow}$ of −2.7 log units. These simulations show that the solvent structure of water-saturated octanol is complex with both polar and nonpolar regions, and that there is significant reorganization of the solute and solvent when the polarity of

the solute changes. This solvent structure can have significant implications for solute−solvent interactions and leads polar solutes to bury themselves in the more polar regions of the solvent, while nonpolar solutes tend to reside in the nonpolar regions. An example of this behavior is the mutation of ethylbenzene to phenol. While ethylbenzene was located in a nonpolar region of water-saturated octanol, phenol prefers to associate with the more polar regions of the solvent where it can benefit from hydrogen bonding with both the water and octanol hydroxyl groups. Comparison of the FEP results with calculations using the continuum GB/SA model for water and octanol shows that, for this set of solutes, GB/SA actually gives more accurate estimates of $\Delta\log P_{ow}$ at a very significant savings in computer time.

Acknowledgment. Financial support was provided by the Rohm and Haas Company and the Office of Naval Research.

References and Notes

(1) Carrupt, P.; Testa, B.; Gaillard, P. Computational Approaches to Lipophilicity: Methods and Applications. In *Reviews in Computational Chemistry*; Lipkowitz, K. B., Boyd, D., Eds.; Wiley-VCH: New York, 1997; Vol. 11, pp 241−345.

(2) Hansch, C.; Leo, A. *Exploring QSAR Fundamentals and Applications in Chemistry and Biology*; American Chemical Society: Washington, DC, 1995.

(3) Hansch, C.; Leo, A.; Hoekman, D. *Exploring QSAR: Hydrophobic, Electronic and Steric Constants*; American Chemical Society: Washington, DC, 1995.

(4) Hansch, C.; Leo, A. J. *Substituent Constants for Correlation Analysis in Chemistry and Biology*; Wiley: New York, 1979.

(5) Martin, Y. C. *Quantitative Drug Design: A Critical Introduction*; Marcel Dekker, Inc.: New York, 1978.

(6) Nasal, A.; Sznitowska, M.; Bucinski, A.; Kaliszan, R. *J. Chrom. A* **1995**, *692*, 83−89.

(7) Cramer, C. J.; Truhlar, D. G. Continuum Solvation Models: Classical and Quantum Mechanical Implementations; In *Reviews in Computational Chemistry*; Lipkowitz, K. B., Boyd, D., Eds.; VCH, Inc.: New York, 1995; Vol. 6, pp 1−72.

(8) Tomasi, J.; Persico, M. *Chem. Rev.* **1994**, *94*, 2027−2094.

(9) Tomasi, J.; Bonaccorsi, R.; Cammi, R.; Valle, F. J. O. d. *J. Mol. Struct. (THEOCHEM)* **1991**, *234*, 401−424.

(10) Jorgensen, W. L. *Acc. Chem. Res.* **1989**, *22*, 184−189.

(11) Gilson, M. K.; Sharp, K. A.; Honig, B. *J. Comput. Chem.* **1988**, 9, 327−335.

(12) Klamt, A. *J. Phys. Chem.* **1995**, *99*, 2224−2235.

(13) Qiu, D.; Shenkin, P. S.; Hollinger, F. P.; Still, W. C. *J. Phys. Chem. A* **1997**, *101*, 3005−3014.

(14) Still, W. C.; Tempczyk, A.; Hawley, R.; Hendrickson, T. *J. Am. Chem. Soc.* **1990**, *112*, 6127−6129.

(15) Sangster, *J. Octanol-Water Partition Coefficients: Fundamentals and Physical Chemistry*; Wiley: Chichester, 1997.

(16) DeBolt, S. E.; Kollman, P. A. *J. Am. Chem. Soc.* **1995**, *117*, 5316−5340.

(17) Karaborni, S.; O'Connell, J. P. *Langmuir* **1990**, *6*, 905.

(18) Karaborni, S.; O'Connell, J. P. *J. Phys. Chem.* **1990**, *94*, 2624.

(19) Jonsson, B.; Edholm, O.; Teleman, O. *J. Chem. Phys.* **1986**, *85*, 2259.

(20) Shelley, J.; Watanabe, K.; Klein, M. L. *Int. J. Quantum Chem. Quantum Biol. Symp.* **1990**, *17*, 103−117.

(21) Wendoloski, J. J.; Kimatian, S. J.; Schutt, C. E.; Salemme, F. R. *Science* **1989**, *243*, 636.

(22) Watanabe, K.; Klein, M. L. *J. Phys. Chem.* **1989**, *93*, 6897.

(23) Damodaran, K. V.; Merz, K. M., Jr.; Gaber, B. P. *Biochemistry* **1992**, *31*, 7656.

(24) Damodaran, K. V.; Merz, K. M., Jr. *Langmuir* **1993**, 9, 1179−1183.

(25) Egberts, E.; Berendsen, H. J. C. *J. Chem. Phys.* **1988**, *89*, 3718.

(26) Edholm, O.; Johansson, J. *Eur. Biophys.* **1987**, *14*, 203.

(27) Bassolino-Klimas, D.; Alper, H. E.; Stouch, T. R. *Biochemistry* **1993**, *32*, 12624−12637.

(28) McKinnon, S. J.; Wittenburg, S. L.; Brooks, B. R. *J. Phys. Chem.* **1992**, *96*, 10497.

(29) van der Ploeg, P.; Berendsen, H. J. C. *J. Chem. Phys.* **1982**, *76*, 3271.

(30) Smith, R. N.; Hansch, C.; Elkins, D. *J. Pharm. Sci.* **1975**, *64*, 599.

(31) Flynn, G.-L. *J. Pharm. Sci.* **1971**, *60*, 345.

(32) Burton, D. E.; Clarke, K.; Gray, G. W. *J. Chem. Soc.* **1964**, 1314.

(33) Richards, W. *G. Methods Princ. Med. Chem.* **1996**, *4*, 173−180.

(34) Klopman, G.; Shaomeng, J. L.; Dimayuga, M. *J. Chem. Inf Comput. Sci.* **1994**, *34*, 752−781.

(35) Ghose, A. K.; Crippen, *G.* M. *J. Comput. Chem.* **1986**, 7, 565−577.

(36) Leo, A. *CLOGP*; Daylight Chemical Information Systems, Mission Viejo, CA.

(37) Leo, A. *Chem. Rev.* **1993**, *30*, 1283−1306.

(38) Rekker, R. F.; Mannhold, R. *Calculation of Drug Lipophilicity;* VCH: New York, 1992.

(39) Rekker, R. F.; De Kort, H. M. *Eur. J. Med. Chem. - Chim. Ther.* **1979**, *14*, 479−88.

(40) Bodor, N.; Gabanyi, Z.; Wong, C.-K. *J. Am. Chem. Soc.* **1989**, *111*, 3783−3786.

(41) Bodor, N.; Buchwald, P. *J. Phys. Chem. B* **1997**, *101*, 3404−3412.

(42) Klopman, G.; Namboodiri, K.; Schochet, M. *J. Comput. Chem.* **1985**, *6*, 28−38.

(43) Waller, C. L. *Quant. Struct.-Act. Relat.* **1994**, *13*, 172−176.

(44) Hawkins, G. D.; Liotard, D. A.; Cramer, C. J.; Truhlar, D. G. *J. Org. Chem.* **1998**, *63*, 4305−4313.

(45) Klamt, A.; Jonas, V.; Buerger, T.; Lohrenz, J. C. W. *J. Phys. Chem. A* **1998**, *102*, 5074−5085.

(46) Haeberlein, M.; Brinck, T. *J. Chem. Soc., Perkin Trans. 2* **1997**, 289−294.

(47) Kamlet, M. J.; Doherty, R. M.; Abraham, M. H.; Marcus, Y.; Taft, R. W. *J. Phys. Chem.* **1988**, *92*, 5244−55.

(48) Abraham, M. H.; Chadha, H. S.; Whiting, G. S.; Mitchell, R. C. *J. Pharm. Sci.* **1994**, *83*, 1085−100.

(49) Essex, J. W.; Reynolds, C. A.; Richards, W. G. *J. Am. Chem. Soc.* **1992**, *114*, 3634−3639.

(50) Essex, J. W.; Reynolds, C. A.; Richards, W. G. *J. Chem. Soc., Chem. Commun.* **1989**, 1152−1154.

(51) Eksterowicz, J. E.; Miller, J. L.; Kollman, P. *A. J. Phys. Chem. B* **1997**, *101*, 10971−10975.

(52) Jorgensen, W. L.; Briggs, J. M.; Contreras, M. L. *J. Phys. Chem.* **1990**, *94*, 1683−1686.

(53) Kollman, P. A.; Merz, K. M., Jr. *Acc. Chem. Res.* **1990**, *23*, 246.

(54) Orozco, M.; Colominas, C.; Luque, F. J. *Chem. Phys.* **1996**, *9*, 209.

(55) Dunn, W. J., III; Nagy, P. I.; Collantes, E. R. *J. Am. Chem. Soc.* **1991**, *113*, 7898−7902.

(56) Dunn, W. J., III ; Nagy, P. I. *J. Comput. Chem.* **1992**, *13*, 468−477.

(57) Maben, S.; Arlt, W.; Klamt, A. *Chem.-Ing.-Tech.* **1995**, *67*, 476.

(58) Giesen, D. J.; Gu, M. Z.; Cramer, C. J.; Truhlar, D. G. *J. Org. Chem.* **1996**, *61*, 8720−8721.

(59) Giesen, D. J.; Chambers, C. C.; Cramer, C. J.; Truhlar, D. G. *J. Phys. Chem. B* **1997**, *101*, 2061−2069.

(60) Giesen, D. J.; Chambers, C. C.; Cramer, C. J.; Truhlar, D. G. *J. Phys. Chem., B* **1997**, *101*, 5084−5088.

(61) Hawkins, G. D.; Cramer, C. J.; Truhlar, D. G. *J. Phys. Chem. B* **1998**, *102*, 3257−3271.

(62) Best, S. A.; Merz, K. M., Jr.; Reynolds, C. H. *J. Phys. Chem. B* **1997**, *101*, 10479−10487.

(63) Reynolds, C. H. *J. Chem. Inf. Comput. Sci.* **1995**, *35*, 738−742.

(64) Jorgensen, W. L.; Tirado-Rives, J. *J. Am. Chem. Soc.* **1988**, *110*, 1657−1666.

(65) Jorgensen, W. L.; Chandrasekhar, J.; Madura, J.; Impey, R. W.; Klein, M. L. *J. Chem. Phys.* **1983**, *79*, 926.

(66) Kollman, P. A. *Chem. Rev.* **1993**, *93*, 2395−2417.

(67) Bash, P. A.; Singh, U. C.; Langridge, R.; Kollman, P. A. *Science* **1987**, *236*, 564−569.

(68) Mezei, M.; Beveridge, D. L. *Ann. N.Y. Acad. Sci.* **1986**, *482*, 1.

(69) Straatsma, T. P.; McCammon, J. A. *Ann. Rev. Phys. Chem.* **1992**, *43*, 407−435.

(70) Cornell, W. D.; Cieplak, P.; Bayly, C. I.; Gould, I. R.; Merz, K. M., Jr.; Ferguson, D. F.; Spellmeyer, D. C.; Fox, T.; Caldwell, J. W.; Kollman, P. A. *J. Am. Chem. Soc.* **1995**, *117*, 5179−5197.

(71) Jorgensen, W. L.; Swenson, C. J. *J. Am. Chem. Soc.* **1985**, *107*, 569−578.

(72) Jorgensen, W. L.; Laird, E. L.; Nguyen, T. B.; Tirado-Rives, J. *J. Comput. Chem.* **1993**, *14*, 206−215.

(73) Jorgensen, W. L. *J. Phys. Chem.* **1986**, *90*, 1276−1284.

(74) Briggs, J. M.; Matsui, T.; Jorgensen, W. L. *J. Comput. Chem.* **1990**, *11*, 958−971.

(75) Vincent, J. J.; Merz , K. M., Jr. *J. Comput. Chem.* **1995**, *16*, 1420−1427.

(76) Cheng, A.; Merz, K. M., Jr. *J. Phys. Chem.* **1996**, *100*, 1927−1937.

(77) Gunsteren, W. F. v.; Berendsen, H. J. C. *Mol. Phys.* **1977**, *34*, 1311−1327.

(78) Ryckaert, J. P.; Ciccotti, G.; Berendsen, H. J. C. *J. Comput. Phys.* **1977**, *23*, 327−341.

(79) Cornell, W. D.; Cieplak, P.; Bayly, C. I.; Kollman, P. A. *J. Am. Chem. Soc.* **1993**, *115*, 9620.
(80) Bayley, C. I.; Cieplak, P.; Cornell, W. D.; Kollman, P. A. *J. Phys. Chem.* **1993**, *97*, 10269−10280.
(81) Besler, B. H.; Merz, K. M., Jr.; Kollman, P. A. *J. Comp. Chem.* **1990**, *11*, 431−439.
(82) Merz, K. M., Jr. *J. Comp. Chem.* **1992**, *13*, 749−767.
(83) Jorgensen, W. L.; Nguyen, T. B. *J. Comput. Chem.* **1993**, *14*, 195−205.
(84) Pearlman, D. A.; Case, D. A.; Caldwell, J. C.; Seibel, G. L.; Singh, U. C.; Weiner, P.; Kollman, P. A. *AMBER 4.1;* Pearlman, D. A., Case, D. A., Caldwell, J. C., Seibel, G. L., Singh, U. C., Weiner, P., Kollman, P. A., Eds.; University of California: San Francisco, 1993.
(85) Berendsen, H. J. C.; Postma, J. P. M.; Gunsteren, W. F. v.; DiNola, A. D.; Haak, J. R. *J. Chem. Phys.* **1984**, *81*, 3684−3690.
(86) We have reparameterized the original water model in order to give better free energies of solvation when used in conjunction with the Merck molecular force field. Best, S. A.; Reynolds, C. H.; Merz, K. M., Jr. Unpublished results.
(87) Reynolds, C. H.; Best, S. A. *CHEMTECH* **1998**, *28*, 28−35.
(88) Allen, M. P.; Tildesley, D. J. *Computer Simulations of Liquids*; Oxford University Press Inc.: New York, 1994.
(89) *89) Phys. Chem. Rev. Data* **1973**, 2.
(90) Iwahashi, M.; Hayashi, Y.; Hachiya, N.; Matsuzawa, H.; Kabayashi, A. *J. Chem. Soc., Faraday Trans.* **1993**, *89*, 707.
(91) Mills, R. *J. Phys. Chem.* **1973**, *77*, 685−8.
(92) Grunwald, E.; Pan, K. C. *J. Phys. Chem.* **1976**, *80*, 2929.
(93) Fletcher, A. N.; Heller, C. A. *J. Phys. Chem.* **1967**, *71*, 3742.
(94) Dannhauser, W. J. *J. Chem. Phys.* **1968**, *48*, 1918.
(95) Karachewski, A. M.; McNiel, M. M.; Eckert, C. A. *Ind. Eng. Chem. Res.* **1989**, *28*, 315.
(96) Shinomiya, T. *Bull. Chem. Soc. Jpn.* **1989**, *62*, 2258.
(97) DeBolt, S. E.; Pearlman, D. A.; Kollman, P. A. *J. Comput. Chem.* **1994**, *15*, 351−373.
(98) Kollman, P. A. *Acc. Chem. Res.* **1996**, *29*, 461.
(99) Morgantini, P.; Kollman, P. A. *J. Am. Chem. Soc.* **1995**, *117*, 6057.
(100) Bernazzani, L.; Cabani, S.; Conti, G.; Mollica, V. *J. Chem. Soc. Faraday Trans.* **1995**, *91*, 649−655.
(101) Cabani, S.; Conti, G.; Mollica, V.; Bernazzani, L. *J. Chem. Soc. Faraday Trans.* **1991**, *87*, 2433−2442.
(102) Dallas, A. J.; Carr, P. W. *J. Chem. Soc., Perkin Trans.* **1992**, *2*, 2155.
(103) Cramer, C. J.; Truhlar, D. G. *J. Comput.-Aided Mol. Des.* **1992**, *6*, 629−666.
(104) Cabani, S.; Gianni, P.; Mollica, V.; Lepori, L. *J. Solution Chem.* **1981**, *10*, 563−595.
(105) Hine, J.; Mookerjee, P. K. *J. Org. Chem.* **1975**, *40*, 292−298.
(106) Ben-Naim, A.; Marcus, Y. *J. Chem. Phys.* **1984**, *81*, 2016−2027.
(107) Jorgensen, W. L.; Severance, D. L. *J. Am. Chem. Soc.* **1990**, *112*, 4768−4774.
(108) Ravishanker, G.; Mehrotra, P. K.; Mezei, M.; Beveridge, D. L. *J. Am. Chem. Soc.* **1984**, *106*, 4102.
(109) Suzuki, S.; Green, P. G.; Bumgarner, R. E.; Dasgupta, S.; Goddard, W. A., III; Blake, G. A. *Science* **1992**, *257*, 942−945.
(110) Linse, P.; Karlstrom, G.; Jonsson, B. *J. Am. Chem. Soc.* **1984**, *106*, 4906.
(111) Meng, E. C.; Caldwell, J. W.; Kollman, P. A. *J. Phys. Chem.* **1996**, *100*, 2367.
(112) Marten, B.; Kim, K.; Cortis, C.; Friesner, R. A.; Murphy, R. B.; Ringnalda, M. N.; Sitkoff, D.; Honig, B. *J. Phys. Chem.* **1996**, *100*, 11775−11788.
(113) Ding, Y.; Bernard, D. N.; Krough-Jespersen, K.; Levy, R. L. *J. Phys. Chem.* **1995**, *99*, 11575.
(114) Miklavc, A. *J. Chem. Inf. Comput. Sci.* **1998**, *38*, 269−270.
(115) Jorgensen, W. L.; Tirado-Rives, J. *Perspect. Drug Discovery Des.* **1995**, *3*, 123−38.
(116) Nagy, P. I.; Dunn, W. J., III; Nicholas, J. B. *J. Chem. Phys.* **1989**, *91*, 3707−3715.
(117) Halgren, T. A. *J. Comput. Chem.* **1996**, *17*, 490−512, 520−552, 553−586, 587− 615, 616−641.
(118) University, c. C. *MacroModel, version 6.0*, 5.5 ed.; University, c. C., Ed.: New York, 1996.